polymer papers

Comparison between morphology and relaxation processes in partially phase-separated polymer blends

M. L. Fernandez, J. S. Higgins and P. E. Tomlins
Department of Chemical Engineering and Chemical Technology, Imperial College of Science and Technology, London SW7 2AZ, UK
(Received 3 February 1988; revised 13 June 1988; accepted 15 June 1988)

Small-angle light scattering (SALS) was used to investigate the kinetics of spinodal decomposition for a mixture of ethylene–vinyl acetate copolymer (EVA) and solution-chlorinated polyethylene (SCPE). Although SALS did not cover the full wavevector range necessary for our experiments we were able to analyse the spinodal kinetics following Cahn–Hilliard theory. An increase in the chlorine content of the SCPE resulted in a shift of the phase boundary to higher temperatures. Relaxation processes and morphology of the blends were related by comparing kinetic and calorimetric measurements.

(Keywords: polymer blends; spinodal decomposition kinetics; ethylene–vinyl acetate copolymer; solution-chlorinated polyethylene; differential scanning calorimetry)

INTRODUCTION

The interdiffusion of two different polymeric species is a process currently exciting both theoretical and experimental interest. Two physical processes are dependent on interdiffusion—the mixing of a compatible pair at an interface and the demixing of a homogeneous blend when it is heated into a two-phase region on the temperature–composition phase diagram. It is the latter process with which we are concerned in this paper. Perhaps because of the large effort involved in developing the theory behind the kinetics of the phase-separation process[1–8], many recent experimental studies have been concentrated on one model system—polystyrene with poly(vinyl methyl ether). It is well known, however, that the delicate free-energy balances governing miscibility of high-molecular-weight polymers are highly susceptible to the details of the interaction between the polymers. For this reason it seems prudent when exploring the validity of the theoretical models to investigate a number of different blend systems. In this paper we further probe the models by comparing data obtained from observation of the phase-separation process in progress with information obtained by investigating the local composition of samples at the end of the process.

High-molecular-weight polymer blend systems suitable for a study of this kind are uncommon, so that until recently very few blends have been studied. A blend which fulfils the experimental requirements as well as being technologically important is the blend of solution-chlorinated polyethylene (SCPE) with ethylene–vinyl acetate copolymer (EVA). Commercially, EVA copolymer is used to improve the properties of poly(vinyl chloride) (PVC) by acting as a plasticizer. Compatibility in these systems, which exhibit lower critical solution temperatures (*LCST*), is primarily due to specific molecular interactions between the components. The advantages of studying blends containing SCPE rather than PVC is that, unlike PVC, the SCPE is not crystalline and the effect of altering the chlorine content of the SCPE on the phase behaviour of the blend can also be studied.

THEORETICAL BACKGROUND

It is well recognized that many solutions of low-molecular-weight compounds have limits of solubility, and the same is true for polymer blends. Mixtures of polymers, however, tend to exhibit lower critical solution temperatures (*LCST*) rather than upper critical solution temperatures (*UCST*), i.e. they separate into two phases on heating.

If a blend in the one-phase region is heated into the two-phase region, the initially homogeneous mixture will phase-separate following one of two possible mechanisms: if the system is unstable to small concentration fluctuations, phase separation will take place by a spontaneous process called 'spinodal decomposition' (SD); if the system is unstable only to large fluctuations, the mechanism of phase decomposition will be 'nucleation and growth' (NG). Unlike SD this latter mechanism requires an activation energy[9–11].

The most widely used theoretical treatment of the behaviour of a mixture undergoing spinodal decomposition consists of a phenomenological statistical theory based on a diffusion equation. This approach was used by Cahn and Hilliard[1,2,12], who employed a simple linear model which retained only the lowest-order term of the composition dependence of the free energy and is considered to be only applicable to the early stage of spinodal decomposition.

In this theory, for an inhomogeneous mixture of small molecules the time dependence of the static structure factor after the system is quenched into the two-phase region should follow an exponential growth:

$$S(q,t)=S(q,0)\exp[2R(q)t] \qquad (1)$$

0032-3861/89/010003-08$03.00

where $S(q, t)$ is the time-dependent static structure factor, $q \equiv |\boldsymbol{q}| = (4\pi n)/\lambda) \sin(\theta/2)$ is the magnitude of the scattering wavevector, and n is the refractive index of the mixture. The incident-beam wavelength is λ and the scattering angle is θ. The growth rate of the amplitude of the concentration fluctuations, $R(q)$, is given as:

$$R(q) = -Mq^2[(\partial^2 \Delta G_m/\partial\phi^2)_0 + 2Kq^2] \quad (2)$$

where M is mobility, $(\partial^2 \Delta G_m/\partial\phi^2)_0$ is the second derivative of the free energy of mixing, ΔG_m, at the initial composition ϕ_0, and K is a positive coefficient. The theory developed for small molecules can be applied to polymeric systems in the small-q domain, where q is smaller than the inverse chain radius, R_g^{-1}. In the small-q region and at the very early stages of demixing, the growing fluctuations may not be affected significantly either by random thermal noise[3] or by the non-linear terms[13], so that the growth is essentially a diffusion-controlled process and the linearized theory is valid if one can achieve experiments at an early enough stage.

In the spinodal decomposition regime, the mixture is unstable to infinitesimal fluctuations so that $(\partial^2 \Delta G_m/\partial\phi^2)_0$ is negative and hence $R(q)$ is positive for values of q smaller than the critical value q_c. Consequently any infinitesimal fluctuations in amplitude with wavenumber $q < q_c$ can grow. The growth rate is given by $R(q)$[2,4,14].

The linear theory predicts the wavenumber q_m of the composition fluctuations that can grow most rapidly in the spinodal decomposition regime and also the maximum relaxation rate $R(q_m)$. From equation (2):

$$q_m^2 = q_c^2/2 = -(\partial^2 \Delta G_m/\partial\phi^2)_0/4K \quad (3)$$

and

$$R(q_m) = M(\partial^2 \Delta G_m/\partial\phi^2)_0/8K \quad (4)$$

It should be noted that q_m is controlled only by thermodynamics while $R(q_m)$ is controlled also by the transport property M; consequently q_m and $R(q_m)$ are determined by a balance of these two physical factors. The existence of q_m and $R(q_m)$ predicts the existence of a scattering maximum at the scattering angle θ_m (where $q_m = (4\pi n/\lambda)\sin(\theta_m/2)$).

From the intercept of a plot of $R(q)/q^2$ vs. q^2 at $q^2 = 0$ one can estimate the 'apparent diffusion coefficient', D_{app}, as defined from equation (2) as:

$$D_{app} = [R(q)/q^2]|_{q^2 \to 0} = -M(\partial^2 \Delta G_m/\partial\phi^2)_0 \quad (5)$$

For polymer blends we adopt a formalism by de Gennes[4] for incompressible, binary liquids composed of macromolecules. He expressed the free-energy density of a homogeneous mixture, $G(\phi)$, by the Flory–Huggins formula[15]. In the context of the mean-field approximation[15-17], he took into account the 'entropy effect' of local variations in concentration which arise from 'connectivity' of monomeric units. On this basis, $R(q)$ becomes[18]:

$$R(q) = -q^2\Lambda(q)[(\partial^2 \Delta G_m/\partial\phi^2)_0 + (R_{ga}^2\phi_a^{-1}N_a^{-1} + R_{gb}^2\phi_b^{-1}N_b^{-1})q^2/3] \quad (6)$$

where R_{gi}, ϕ_i and N_i are the radius of gyration, volume fraction and degree of polymerization of component i respectively, and $\Lambda(q)$ is the q-dependent Onsager coefficient given by:

$$\Lambda(q) = M(\phi_a^{-1}N_a^{-1} + \phi_b^{-1}N_b^{-1}) \quad \text{for } qR_0 \leqslant 1 \quad (7)$$

R_0 being the unperturbed end-to-end distance of a polymer coil. The Onsager coefficient is related to the classical mobility constant M in the Cahn theory:

$$M = \Lambda(q \to 0)/k_B T \quad (8)$$

where k_B is the Boltzmann constant.

In the literature, values of R_g^2/M_w rather than R_g^2 are found. So, for practical purposes, equation (6) can be modified by simply replacing the term in square brackets by the following expression:

$$\left[\frac{R_{ga}^2}{\phi_a N_a} + \frac{R_{gb}^2}{\phi_b N_b}\right] = M_a\left[\frac{(R_g^2/M_w)_a}{\phi_a} + \frac{(R_g^2/M_w)_b}{\phi_b}\frac{M_b}{M_a}\right] \quad (9)$$

where polydispersity effects or changes in conformation in the blend have been ignored.

These two developments have been compared elsewhere[19]. One important result is that q_m, $\overline{D_{app}}$ and $R(q_m)$ should be proportional to the quench depth $\Delta T = T - T_s$ and at the spinodal point ($T = T_s$) the three quantities should vanish.

As we have mentioned before, Cahn–Hilliard theory is only applicable to the early stages of spinodal decomposition. At later times the kinetics start to deviate from the linear SD kinetics due to Ostwald ripening mechanisms[20]. This latter stage is characterized for the decreasing of q with time, so that the peak of intensity *versus* angle shifts to lower angles with time.

When thermal fluctuations are included, equation (1) is modified and becomes[21]:

$$S(q, t) = S_x(q) + [S(q, 0) - S_x(q)]\exp[2R(q)t] \quad (10)$$

and

$$S_x(q) = -\Lambda q^2/R(q) \quad (11)$$

where $R(q)$ has the same form as in equation (6).

$S_x(q)$ is negative for $q < q_c$ (ref. 22) and for $(T - T_s) > 1$ K so that the concentration fluctuations rapidly overtake and dominate $S_x(q)$. This virtual structure factor must be determined if the contribution of thermal fluctuations in a polymer system which undergoes phase decomposition are to be evaluated. For small quench depths the virtual structure factor may be important for high q values around $q = q_c$ where there is a discontinuity in $S_x(q)$, but it is generally less important for small q values.

The most acceptable demonstration of an SD mechanism is the existence of characteristic spinodal kinetics, i.e. observation of a continuous growth of certain small-amplitude composition modulations. The most widely used technique for kinetic experiments is scattering of radiation; the choice between light (SALS)[23], X-rays (SAXS) or neutrons (SANS) as incident beam depends on the size of the domains that are formed during the phase separation and on the contrast between the phases. For our system preliminary results showed that SALS was the most convenient technique; however, as we will see later, none of the different radiations cover the full q range necessary for studying this mixture.

One of the most commonly used methods for establishing miscibility in polymer–polymer blends or partial phase mixing in such blends is through the determination of the glass transition, or transitions, in the blend *versus* those of the unblended constituents. A miscible polymer blend will generally exhibit a single glass transition at a temperature intermediate between the T_g values of the components.

The dependence of the glass transition temperature of the mixture on the volume fraction is usually explained satisfactorily by the simple Fox equation[24]:

$$1/T_g = \phi_a/T_{ga} + \phi_b T_{gb} \quad (12)$$

where T_{gi} and ϕ_i are the T_g and volume fraction of component i in the mixture, and T_g is the glass transition temperature of the blend.

A phase-separated system will exhibit two T_g values corresponding to the two phases present in the mixture. These two T_g values will be further apart as the difference in composition between the two coexisting phases increases.

EXPERIMENTAL

Chlorinated polyethylenes were prepared by photochlorination. A commercial high-density linear polyethylene (40 g) with a nominal M_n of 1×10^4 was dissolved in chlorobenzene (800 ml, AR grade) at 403 K. The reaction between dry chlorine gas bubbled through the solution (35 ml min^{-1}) was initiated by the light from a 60 W tungsten bulb. The degree of chlorination is dependent on the reaction time. It takes approximately 20 h to produce a chlorine content of 72% by weight with ~50% efficiency. The product was precipitated in 10 times excess of ice-cold methanol, washed twice and then dried under a vacuum of 1 mmHg at 343 K for at least a week.

Chai *et al.*[25] showed by n.m.r. that the chlorines are randomly located along the ethylene chains for chlorine contents greater than 50% by weight.

Near-monodisperse fractions were reproduced by dissolving the SCPE in benzene to form a 2% solution by weight. Propan-2-ol was then added until the solution became turbid. The precipitate was then redissolved by warming the flask to 313 K and then allowing it to cool down slowly. After removal of the supernatant, the fractions were redissolved in benzene and reprecipitated in methanol.

The properties of the SCPEs are listed in *Table 1*. The composition was determined by elemental analysis. The molecular weights were determined by gel permeation chromatography and are relative to polystyrene standards. The T_g measurements were made by using a differential scanning calorimeter (Perkin–Elmer DSC 2).

Ethylene–vinyl acetate copolymer was obtained from ICI Plc (Evatone 45) and fractionated using the same procedure as for the SCPE; the properties of the fractions are also listed in *Table 1*.

Blends of different compositions were prepared by solvent casting. Their characteristics are shown in *Table 2*. Dried Analar methyl ethyl ketone was used as the common solvent for EVA/SCPE. A 15% solution of the two polymers in the desired proportions was made. This solution was then spun using an MSE(25) centrifuge to remove any foreign particles and dust present. Samples for SALS were prepared by pouring enough of the centrifuged polymer blend solution onto clean 19 mm diameter coverslips contained in a Petri dish. Petri dishes excluded dust and gave a slow rate of evaporation of the solvent. The samples were kept at room temperature for 7 days and then were placed in a vacuum oven at 303 K for another week until finally the temperature was raised to 333 K under high vacuum for 1 h immediately before testing.

SALS experiments were performed using a laboratory-built testing rig[26]. The light source was a He–Ne Aerotech model 1105P laser ($\lambda = 633$ nm, 8 mW). The detector consisted of a semicircular array of 32 photodiodes whose angle θ with respect to the sample could be chosen from 0 to 90°. For our experiments, a range from 5 to 67° was selected. The response of each photodiode to light and dark current was normalized by monitoring the intensity recorded by each photodiode after placing an isotropic scatterer in the beam.

The cloud-point curves were estimated by turbidimetry; samples in the one-phase region were heated up into the two-phase region at a rate of 0.2 deg min^{-1} and the scattered light was recorded. The cloud point was taken at the temperature at which the light intensity started to deviate from a straight line.

Kinetic experiments were performed as follows. The sample block and holder were preheated to the desired temperature, the sample holder was withdrawn and the coverslip supporting the polymer film loaded into the holder which was then slid back into the block. The scattered intensity from the polymer blend is monitored as a function of time and a BBC microcomputer was used for sampling photodiode voltages at user selected intervals.

A thermocouple was attached to the sample and this was inserted into the heating block in order to measure the length of time required for the sample to reach the working temperature; this time was of the order of 5–7 s. However, as can be seen clearly from *Figure 1*, even if the sample took 20 s to reach the working temperature, this would only question the accuracy of the first four points in the plot of $\ln I$ vs. q, for which our conclusions would still be valid.

Since the sample has to pass through the metastable region in order to go from the one-phase to the two-phase region, the question might arise whether the blend develops a structure which is due not purely to spinodal decomposition but also to nucleation and growth. However, it is well known that the process of nucleation is rather slow and consequently the temperature jump in our experiments is too quick to allow any development of a structure characteristic of the metastable region.

Calorimetric measurements were performed in a Perkin–Elmer DSC-2C differential scanning calorimeter. All scanning data were taken at 20°C min^{-1} heating rates on samples in crimp-sealed aluminium cups. A few milligrams of sample were placed in the cups. Two-phase

Table 1 Characteristics of the EVA copolymer and the SCPEs used in this work

Polymer	M_n	M_w	*PD*	T_g (K)	Refractive index	Cl (%)	Acetate (%)
SCPE56	6.18×10^4	1.87×10^5	3.02	321	1.51	56	–
SCPE51	5.37×10^4	6.75×10^4	1.28	290	1.51	51	–
EVA45	4.0×10^5	1.33×10^6	3.33	253	1.42	–	45

Table 2 Compositions of the eight different blends studied in this work

Code	EVA45 (%)	SCPE56 (%)	SCPE51 (%)
56-1	30	70	–
56-2	41	59	–
56-3	51.5	48.5	–
56.4	57	43	–
51-1	51	–	49
51-2	57	–	43
51-3	65	–	35
51-4	75	–	25

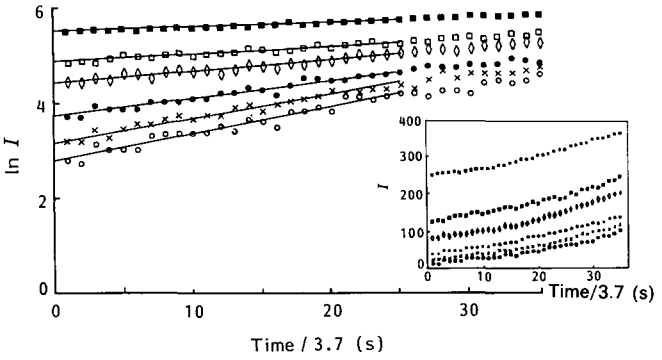

Figure 1 Logarithm of the scattered light intensity plotted against a linear timescale for an EVA45/SCPE56 blend containing 41% EVA45, after initiation of isothermal phase separation at 430 K for different q values: (○) $q=0.53\times10^5\,cm^{-1}$, (×) $q=0.73\times10^5\,cm^{-1}$, (●) $q=0.92\times10^5\,cm^{-1}$, (◇) $q=1.11\times10^5\,cm^{-1}$, (□) $q=1.39\times10^5\,cm^{-1}$, (■) $q=1.52\times10^5\,cm^{-1}$. Inset: variation of the scattered light intensity with time, for the same experiment

blends were achieved by annealing at temperatures above their spinodal temperatures and quenching. In this way, samples of the four different compositions were phase-separated at different temperatures over different lengths of time.

RESULTS

Kinetic results

The inset in *Figure 1* shows typical variations of the scattered light intensity of the samples as a function of time for different angles after initiation of isothermal phase separation of a blend containing 59% of SCPE56 at 430 K.

In *Figure 1* logarithms of the light intensity are plotted against a linear timescale. It is clearly seen that the scattered intensity increases exponentially with time in the early stages of phase separation, in agreement with the theoretical prediction of Cahn and Hilliard for spinodal decomposition. From the slope of these plots one can measure the relaxation rate $R(q)$ as a function of the wavenumber q.

Figure 2 shows results for $R(q)$ as a function of q estimated for the same sample. $R(q)$ should increase with q to reach a maximum at a particular value q_m and then decrease with further increase of q. In the accessible q range, $R(q)$ increases with increasing q over the whole range thus corresponding to the regime where the kinetics are dominantly controlled by the transport phenomenon, i.e. by the term Mq^2 rather than the thermodynamic term $[-(\partial^2\Delta G_m/\partial\phi^2)_0-2Kq^2]$ in equation (2).

Figure 3 shows a typical plot of $R(q)/q^2$ vs. q^2; a fairly good linear relationship was obtained experimentally except at very low q values, indicating that the early stages of SD for the sample under investigation can be well described by the linear SD theory. From plots such as *Figure 3* one can estimate the characteristic parameters describing the dynamics of the phase separation. The 'apparent diffusion coefficient' $\overline{D_{app}}$ is given by the intercept of $R(q)/q^2$ vs. q^2 at $q^2=0$. The 'most probable wavenumber' of growing fluctuations at the highest rate, q_m (equation (3)), is obtained from the ratio of slope to intercept, and the 'most probable growth rate' of these fluctuations, $R(q_m)$ (equation (4)), is given by the ratio of the squared slope to four times the intercept.

The parameters are summarized in *Table 3*, where d_m represents the most rapidly growing size:

$$d_m=2\pi/q_m \qquad (13)$$

t_m is the point up to which we have fitted our $\ln I$ vs. t plots, i.e. the point up to which we observe an exponential behaviour of the intensity as a function of time. This time, t_m increases noticeably as the quench depth decreases.

It can be seen that an increase in temperature (i.e. an increase in the thermodynamic driving force for the phase separation) involves an increase in $\overline{D_{app}}$, q_m^2 and $R(q_m)^{1/2}$. These three quantities should vanish at the spinodal point $T=T_s$.

Figure 4 shows a typical plot of $\overline{D_{app}}$ as a function of temperature for a 70% SCPE56 composition. A fairly good linear relationship was obtained in all the cases from which the spinodal points were estimated. The inset in *Figure 4* represents the spinodal curve obtained following this extrapolation procedure, for the systems EVA45/SCPE51 with open circles and EVA45/SCPE56 with filled circles. The study of the second system will be discussed later. Unfortunately, owing to experimental

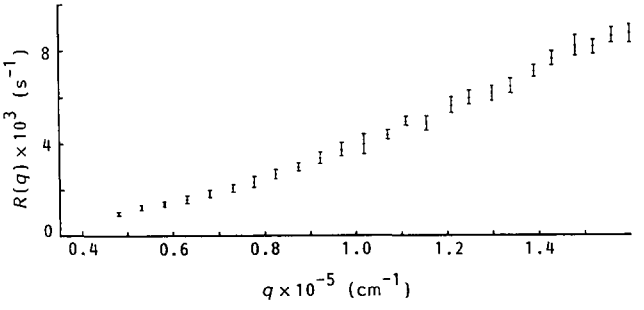

Figure 2 Variation of the relaxation rate $R(q)$ as a function of q as in *Figure 1*

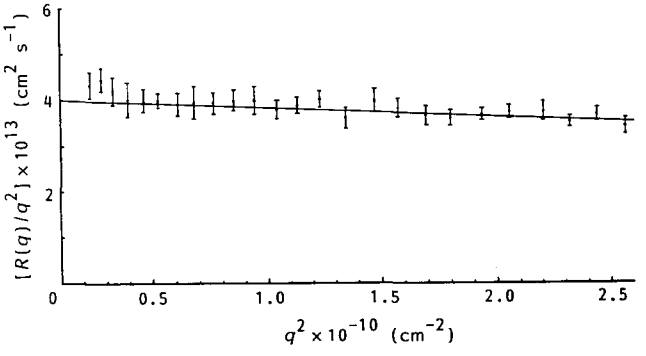

Figure 3 Plot of $R(q)/q^2$ vs. q^2 for the same temperature-jump experiment

Table 3 Thermodynamic parameters obtained for the system EVA45/SCPE56

(a) System 56-1, 30% EVA45/70% SCPE56, $T_s = 402.25 \pm 1.6$ K

T (K)	$\overline{D_{app}} \times 10^{13}$ ($cm^2\ s^{-1}$)	$q_m \times 10^{-5}$ (cm^{-1})	$d_m \times 10^5$ (cm)	$R(q_m) \times 10^4$ (s^{-1})	t_m (s)
431.4	6.1±0.55	2.56±0.11	2.45±0.11	199.2±35.6	63
430.6	6.1±1.93	2.39±0.35	2.63±0.45	174.5±110	63
429.9	5.6±1.25	2.05±0.22	3.06±0.36	117.7±58.4	63
423.1	3.9±0.41	2.21±0.11	2.84±0.15	95.1±21.0	148
421.0	4.0±0.31	1.94±0.13	3.24±0.22	108.0±49.4	185
413.0	1.98±0.13	1.36±0.04	4.62±0.15	18.5±2.6	236

(b) System 56-2, 41% EVA45/59% SCPE56, $T_s = 401.25 \pm 1.6$ K

T (K)	$\overline{D_{app}} \times 10^{13}$ ($cm^2\ s^{-1}$)	$q_m \times 10^{-5}$ (cm^{-1})	$d_m \times 10^5$ (cm)	$R(q_m) \times 10^4$ (s^{-1})	t_m (s)
431.2	5.7±0.28	1.97±0.05	3.18±0.08	111.0±11.5	96
428.0	4.42±0.26	1.89±0.06	3.32±0.10	79.6±9.6	111
423.1	3.5±0.20	1.84±0.05	3.42±0.09	58.9±6.9	126
418.1	2.24±0.02	1.54±0.003	4.08±0.01	26.4±0.5	143
410.1	1.5±0.12	1.17±0.04	5.39±0.21	10.2±1.7	207

(c) System 56-3, 51.5% EVA45/48.5% SCPE56, $T_s = 400.0 \pm 1.0$ K

T (K)	$\overline{D_{app}} \times 10^{13}$ ($cm^2\ s^{-1}$)	$q_m \times 10^{-5}$ (cm^{-1})	$d_m \times 10^5$ (cm)	$R(q_m) \times 10^4$ (s^{-1})	t_m (s)
434.2	9.69±0.72	1.56±0.06	4.03±0.15	117.9±8.4	37
431.3	9.63±0.31	1.32±0.02	4.76±0.06	83.5±5.5	48
427.2	7.98±0.23	1.27±0.02	4.95±0.06	64.0±3.7	63
408.0	1.8±0.30	1.24±0.10	5.06±0.38	13.8±5.1	215

(d) System 56-4, 57% EVA45/43% SCPE56, $T_s = 396.0 \pm 1.2$ K

T (K)	$\overline{D_{app}} \times 10^{13}$ ($cm^2\ s^{-1}$)	$q_m \times 10^{-5}$ (cm^{-1})	$d_m \times 10^5$ (cm)	$R(q_m) \times 10^4$ (s^{-1})	t_m (s)
434.1	5.57±0.75	2.10±0.11	2.99±0.15	120.1±34.7	33
431.2	4.0±0.19	1.88±0.04	3.34±0.07	70.5±7.4	96
427.1	4.19±0.19	1.48±0.03	4.25±0.09	45.8±4.2	104
423.0	3.13±0.19	1.60±0.05	3.93±0.12	40.2±5.0	130
418.1	2.19±0.18	1.76±0.07	3.57±0.14	34.0±5.8	155
413.0	1.84±0.05	1.44±0.02	4.37±0.05	19.0±1.1	370
408.0	1.34±0.06	1.30±0.03	4.82±0.11	11.4±1.1	334

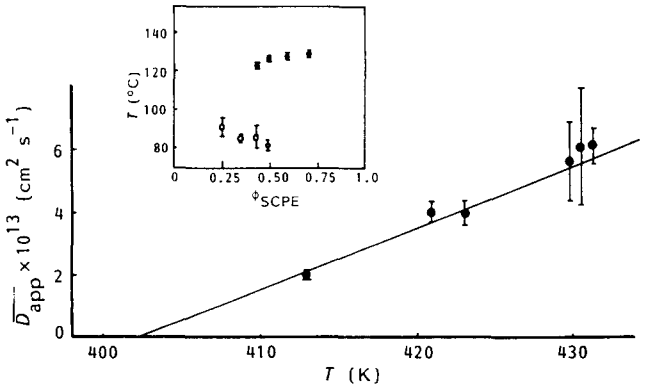

Figure 4 Apparent diffusion coefficient $\overline{D_{app}}$ vs. temperature T for the same experiment. Inset: spinodal curves for the EVA45/SCPE56 system with filled circles, and EVA45/SCPE51 with empty circles, obtained from the intercept of plots of $\overline{D_{app}}$ vs. T at $\overline{D_{app}} = 0$

limitations it was very difficult to perform kinetic experiments outside the reported range, so that the spinodal curves are not complete. These phase boundaries present a rather peculiar shape, as can be seen in the inset of *Figure 4*: while the EVA45/SCPE56 curve seems to indicate that the location of the critical point would be shifted towards lower SCPE compositions, the shape of the EVA45/SCPE51 phase diagram seems to point towards a critical point closer to higher SCPE compositions. However, this result is not surprising since both SCPEs have different chlorine contents, which influences the polymer–polymer interactions and results, among other effects, in the shifting of the critical point. This result agrees with those obtained by Rostami[27] for mixtures of EVA and SCPEs and by Chai[28] for mixtures of poly(butyl acrylate) with SCPE.

Typical plots of the three magnitudes $\overline{D_{app}}$, $R(q_m)^{1/2}$ and q_m^2 as a function of the quench depth ΔT are shown in *Figure 5*. From these plots it is clear that the experimental results for these three magnitudes are in very good agreement with the theory, and a unique linear relationship is obvious from the data.

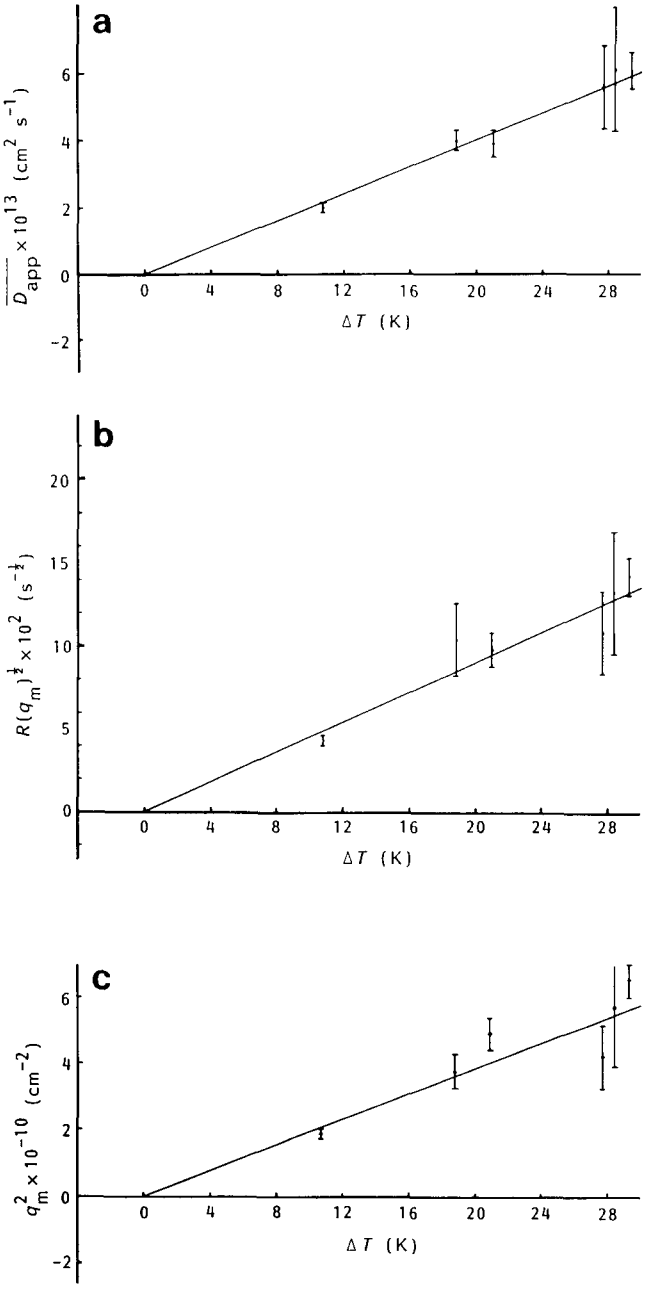

Figure 5 (a) Apparent diffusion coefficient $\overline{D_{app}}$, (b) square root of the maximum growth rate $R(q_m)^{1/2}$ and (c) squared maximum wavenumber q_m^2 against quench depth $\Delta T = T - T_s$ as in *Figure 1*

From *Table 3* it is clearly seen that d_m increases as the temperature decreases. By using the Flory–Huggins expression for the Gibbs free energy of mixing and after several very simple mathematical operations we obtain the result that[29]:

$$d_m \propto [(T/T_s) - 1]^{-1/2} \quad (14)$$

where T_s is the spinodal temperature at the original composition.

Thus, a plot of $\ln d_m$ vs. $\ln(T - T_s)$ should be a straight line with slope equal to -0.5. *Figure 6* represents this plot for the systems 56-1 and 56-2 where the spinodal temperatures were taken as those depicted in *Table 3*. Very good linear relationships were obtained with slopes -0.52 and -0.48, which agree very well with the predicted value, -0.5.

Another interesting result is the large particle sizes obtained in the phase-separated samples, in the range 2000–5000 Å. These values explain the fact that we can detect two phases in the d.s.c. experiments for samples phase-separated only for 20 s, as we will see later.

As already remarked, on the plots of $R(q)$ vs. q (as in *Figure 2*), the growth rate values appear to increase towards a maximum although they never reach it. The same behaviour is observed in the plots of intensity vs. q. However, when the same data are replotted as $R(q)/q^2$ vs. q^2, the q_m values in *Table 3* can be obtained for each plot as explained earlier.

Table 3 shows that the q_m values deduced from our plots are greater than the highest value of q covered in our experiments and thus these results seem to indicate that the values of q_m lie outside the range of q accessible in our experimental set-up.

In order to support this argument we performed both SALS and SANS studies on similar 75/25 EVA45/SCPE56 samples. With the first sample we studied, by SALS, the kinetics of phase demixing at 430 K and the results were analysed as described above. Following this treatment we obtained a linear relationship of $\ln I$ vs. time up to $t = 92$ s. as can be seen in the inset of *Figure 7*, and a predicted value of $q_m = 3.54 \times 10^3$ Å^{-1}. A similar sample was annealed at the same temperature for 92 s and quenched immediately to below room temperature. Small-angle neutron scattering experiments were then performed on the sample in the ILL neutron facility in Grenoble. *Figure 7* shows the plot obtained for intensity vs. q, and it clearly shows a maximum at a q value which agrees remarkably well with that predicted from SALS experiments.

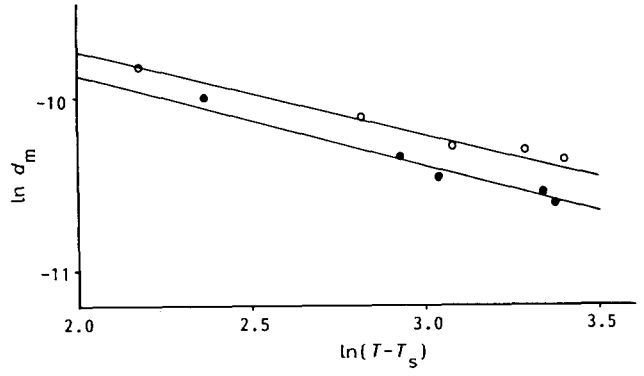

Figure 6 Logarithm of the fastest growing size (d_m) for two EVA45/SCPE56 compositions (70% and 59% in SCPE56) against the logarithm of $T - T_s$ taking $T_s = 402.25$ and 401.25 K respectively

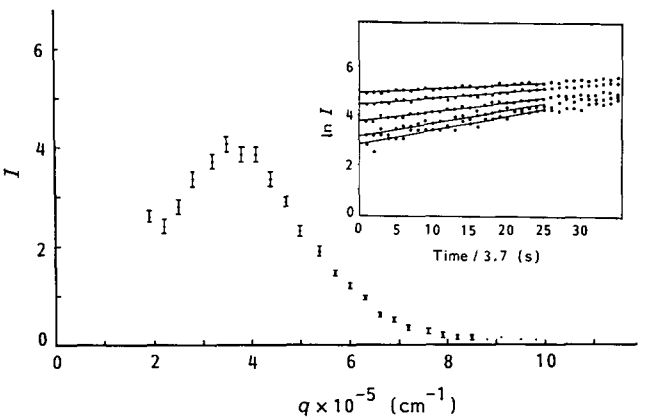

Figure 7 Intensity scattered by a 75/25 EVA45/SCPE56 blend annealed for 92 s at 430 K and quenched into the one-phase region plotted against q as measured by SANS. Inset: plot of logarithm of intensity vs. time for a similar sample, for different scattering angles obtained from SALS kinetic experiments (scattering angles θ are, from top, 29°, 37°, 45°, 57° and 63°)

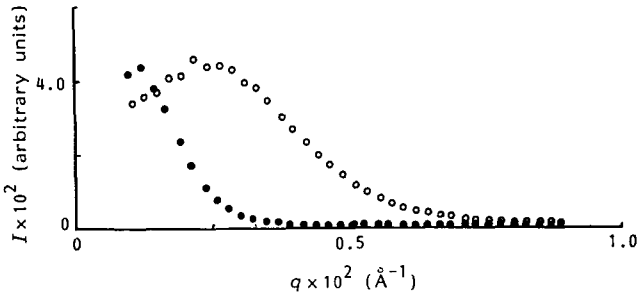

Figure 8 Scattered intensity plotted against q for similar 50/50 EVA45/SCPE51 annealed and quenched samples. Sample A (○) was annealed for 15 min at 380 K and sample B (●) was phase-separated at the same temperature for 4 h

In our kinetic experiments we also measured the scattered intensity vs. q as a function of temperature. Although shallow peaks were obtained in some cases, late stages are not observed even after running the samples for up to 8 h, i.e. the peak did not move to lower q.

In order to investigate whether late stages occur in our system we performed SANS experiments on two 50/50 EVA45/SCPE51 identical samples, A and B. We annealed both of them at 380 K, but sample A was phase-separated for 15 min and sample B for 4 h. From *Figure 8* it is clearly seen that the peak in intensity vs. q moves towards smaller q values with increasing annealing time as expected in the late stages. The reason why we cannot observe these stages from SALS experiments is that the peaks are outside the light scattering range.

From these results it can also be seen that the peaks we have observed in some cases in SALS experiments at very long annealing times correspond to the very late stages of spinodal decomposition when the peaks have moved so far to lower q that we can detect them in the light q range.

In order to study the influence of the chlorine content of the SCPE on the phase behaviour we performed similar experiments on a second system, EVA45/SCPE51. Four different compositions were prepared; their characteristics are shown in *Table 2*. The analysis of the data was carried out in a similar way to the EVA45/SCPE56 system and the results are summarized in *Table 4*.

Several conclusions can be deduced by comparing the

Table 4 Thermodynamic parameters obtained from the system EVA45/SCPE51

(a) System 51-1, 51% EVA45/49% SCPE51, $T_s = 353.7 \pm 3.4$ K

T (K)	$\overline{D_{app}} \times 10^{13}$ ($cm^2 s^{-1}$)	$q_m \times 10^{-5}$ (cm^{-1})	$d_m \times 10^5$ (cm)	$R(q_m) \times 10^4$ (s^{-1})	t_m (s)
372.9	2.37±0.13	2.10±0.11	2.99±0.15	40.4±4.44	325
369.6	1.88±0.17	2.12±0.09	2.96±0.12	42.2±8.2	382
365.6	1.41±0.07	2.19±0.01	2.87±0.02	33.8±0.33	403
362.6	1.04±0.05	2.12±0.01	2.96±0.15	23.4±0.23	580
357.8	0.54±0.001	1.89±0.004	3.32±0.003	9.7±0.03	1155

(b) System 51-2, 57% EVA45/43% SCPE51, $T_s = 356.3 \pm 6.7$ K

T (K)	$\overline{D_{app}} \times 10^{13}$ ($cm^2 s^{-1}$)	$q_m \times 10^{-5}$ (cm^{-1})	$d_m \times 10^5$ (cm)	$R(q_m) \times 10^4$ (s^{-1})	t_m (s)
373.0	1.80±0.07	1.65±0.03	3.81±0.07	24.5±2.0	381
367.7	1.11±0.01	1.73±0.01	3.63±0.02	16.7±0.2	515
362.9	0.63±0.02	1.92±0.03	3.27±0.05	11.6±0.8	689
362.7	0.68±0.10	2.03±0.15	3.10±0.20	14.1±4.5	591

(c) System 51-3, 65% EVA45/35% SCPE51, $T_s = 358.6 \pm 0.6$ K

T (K)	$\overline{D_{app}} \times 10^{13}$ ($cm^2 s^{-1}$)	$q_m \times 10^{-5}$ (cm^{-1})	$d_m \times 10^5$ (cm)	$R(q_m) \times 10^4$ (s^{-1})	t_m (s)
372.9	2.58±0.20	1.87±0.07	3.36±0.12	45.2±0.5	188
367.6	1.60±0.09	1.93±0.06	3.26±0.10	29.9±3.6	204
362.7	0.74±0.02	3.46±0.03	1.82±0.02	44.2±1.8	278

(d) System 51-4, 75% EVA45/25% SCPE51, $T_s = 363.8 \pm 5.2$ K

T (K)	$\overline{D_{app}} \times 10^{13}$ ($cm^2 s^{-1}$)	$q_m \times 10^{-5}$ (cm^{-1})	$d_m \times 10^5$ (cm)	$R(q_m) \times 10^4$ (s^{-1})	t_m (s)
373.9	1.24±0.08	1.99±0.06	3.16±0.10	24.6±5.9	95
372.8	1.05±0.17	2.29±0.02	2.74±0.02	27.7±9.1	167
369.8	0.67±0.04	1.48±0.04	4.25±0.12	7.3±0.2	206
369.7	0.65±0.06	1.39±0.06	4.52±0.19	6.3±1.2	138
366.8	0.35±0.07	2.02±0.14	3.11±0.02	7.1±2.0	256

data obtained for the two systems: For the same quench depth the resulting $\overline{D_{app}}$ values for the system EVA45/SCPE56 are smaller than those corresponding to the system EVA45/SCPE51. The data also show much smaller spinodal temperatures for the EVA45/SCPE51 system. These are the expected behaviours and agree well with previously published results[30]. The system EVA45/SCPE56 has a much higher phase boundary because the SCPE56 provides a higher concentration of interacting groups than the SCPE51, resulting in a higher degree of compatibility. This effect is also attributed to the reduced mobility of the EVA45/SCPE56 system compared to that of the SCPE51/EVA45 blend due to the difference in the value of T_g for both SCPEs. The comparison between the spinodal curves for the two systems is depicted in the inset in *Figure 4*.

The second conclusion is that the q_m values for each composition do not change much with temperature. In order to explain this result we have to refer to equations (13) and (14) from which a dependence $q_m \propto \Delta T^{1/2}$ is deduced. This means that the change of q_m with quench depth is sharp for small ΔT values but soon levels off. In our experiments the smallest values of the quench depths are 3 K for the EVA45/SCPE51 system and 8 K for the EVA45/SCPE56 system. Thus we cannot expect dramatic changes in the q_m values obtained.

D.s.c. measurements

Three sets of experiments were performed. In the first set of experiments, samples in the one-phase region were analysed in order to determine the T_g values of the blends for the different compositions. The second group of samples were phase-separated at the same temperature over different lengths of time. Finally, a third set of experiments was carried out by phase-separating a group of samples at different temperatures for the same length of time.

All the samples in the one-phase region showed a single T_g intermediate between the two T_g values of the pure homopolymers. As expected, the T_g values moved to higher values as the composition in SCPE increased.

For all the scans in the two-phase region two T_g values were obtained and the thermograms show that for a fixed temperature the two T_g values are more separated as the length of time of phase separation increases. *Figure 9* shows a typical result for a 43% composition in SCPE56 in the one-phase region and after having annealed the samples at 399 K for 20, 30 and 360 s.

Figure 10 shows the d.s.c. results for a 70% SCPE56 sample in the one-phase region and after having been annealed for 25 s at three different temperatures: 431.4, 413 and 406 K. It is clearly shown that an increase in the

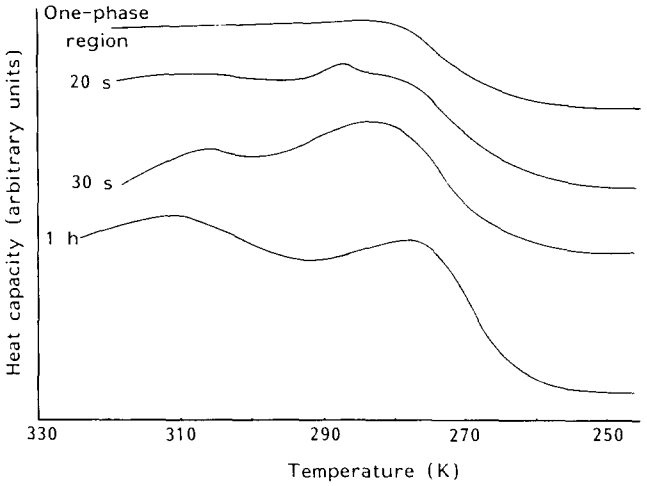

Figure 9 D.s.c. thermograms for EVA45/SCPE56 (43% in SCPE56) composition, in the one-phase region and after annealing at 399 K for 20, 30 and 360 s

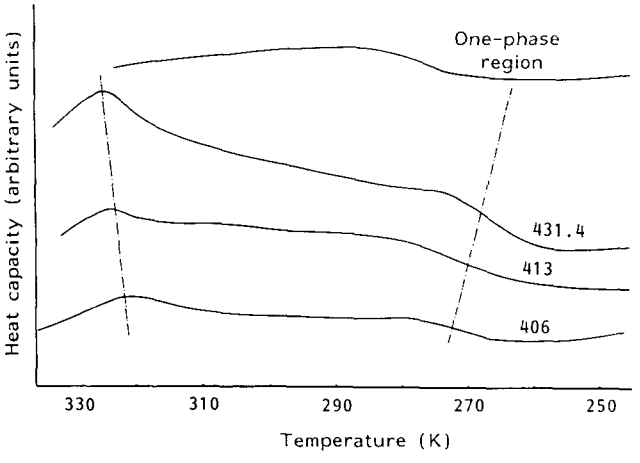

Figure 10 D.s.c. thermograms for EVA45/SCPE56 (70% in SCPE) composition, in the one-phase region and after annealing for 25 s at 431.4, 413 and 406 K

annealing temperature results in a wider separation between the two T_g values obtained in each case.

This result is to be expected if we remember the shape of the Gibbs free energy vs. composition curve. As the temperature increases the points of minimum free energy shift towards the two sides of the diagram and the unstability and metastability region widens. The two final compositions reached by the samples that are phase-separating are more distant at higher temperatures, which results in a wider separation between the two T_g values obtained in each case.

From these d.s.c. results it is possible to deduce information about which phase demixing mechanism is taking place in the blends studied. From *Figures 9* and *10* it is clear that the phase-separation process that is taking place in our experiments is continuous. The gap between the compositions of the two phases formed in the systems increases smoothly either with time or with temperature. This is one of the most outstanding characteristics of the spinodal decomposition mechanism which clearly distinguishes it from nucleation and growth.

CONCLUSIONS

Small-angle light scattering is a suitable technique for studying the spinodal decomposition kinetics of the EVA/SCPE blends.

It is possible to analyse the spinodal decomposition kinetics of these blends using the Cahn–Hilliard theory.

We have obtained the spinodal and not the binodal curve since we have observed peaks in the scattered intensity vs. q. Unfortunately these peaks are in between the q ranges accessible by small-angle light and neutron scattering.

Late stages of spinodal decomposition occur at relatively high annealing times.

An increase in the chlorine content of the SCPE results in a higher degree of interaction within the blend and to a lower mobility of the mixture, which shifts the phase boundary to higher temperatures.

Relaxation processes and morphology of the blends can be related by comparing kinetic and d.s.c. results. As we progress along the spinodal decomposition process the samples that initially showed a single T_g present two T_g values that are more separated as we anneal them for longer periods at a fixed temperature or at increasing temperatures during the same length of time. They reach a final state corresponding to the compositions with the lowest free energy available to the system.

ACKNOWLEDGEMENTS

The authors thank J. Clark, H. Fruitwala and Dr A. Rennie who carried out the neutron scattering experiments, Dr R. Hill for the preparation of the SCPEs and EVA and the Excelentisima Diputacion de Vizcaya–Bizkai Foru Aldundia for financial support.

REFERENCES

1 Cahn, J. W. and Hilliard, J. E. *J. Chem. Phys.* 1958, **28**, 258
2 Cahn, J. W. and Hilliard, J. E. *J. Chem. Phys.* 1959, **31**, 688
3 Cook, H. E. *Acta Metall.* 1970, **18**, 297
4 de Gennes, P. G. *J. Chem. Phys.* 1980, **72**, 4756
5 Pincus, P. *J. Chem. Phys.* 1981, **75**, 1966
6 Brochard, F., Jouffroy, J. and Levinson, P. *Macromolecules* 1983, **16**, 1638
7 Kramer, E. J., Green, P. and Palmstrom, C. J. *Polymer* 1984, **25**, 473
8 Binder, K. *J. Chem. Phys.* 1983, **79**, 6387
9 Cahn, J. W. *Trans. Metall. Soc. AIME* 1968, **242**, 166
10 Kaplan, D. S. *J. Appl. Polym. Sci.* 1976, **20**, 2615
11 Krause, S. *J. Macromol. Sci.* (C) 1972, **7**, 251
12 Cahn, J. W. *Acta Metall.* 1961, **9**, 795
13 Langer, J. S., Bar-on, M. and Miller, H. D. *Phys. Rev.* (A) 1975, **11**, 1417
14 Cahn, J. W. *J. Chem. Phys.* 1965, **42**, 93
15 Flory, P. J. 'Principles of Polymer Chemistry', Cornell University Press, Ithaca, NY, 1953
16 Scott, R. L. *J. Chem. Phys.* 1949, **17**, 268
17 Tompa, H. 'Polymer Solutions', Butterworths, London, 1956
18 Higgins, J. S., Fruitwala, H. and Tomlins, P. E. *Makromol. Chem. Macromol. Symp.* 1988, **16**, 313
19 Hashimoto, T., Kumaki, J. and Kawai, H. *Macromolecules* 1983, **16**, 641
20 Siggia, E. D. *Phys. Rev.* (A) 1979, **20**(2), 595
21 Okada, M. and Han, C. C. *J. Chem. Phys.* 1986, **85**(9), 5317
22 Meier, H. and Strobl, G. R. *Macromolecules* 1987, **20**, 649
23 Voight-Martin, I. G. *Adv. Polym. Sci.* 1985, **67**, 195
24 Fox, T. G. *Bull. Am. Phys. Soc.* 1956, **2**, 123
25 Chai, Z., Shi, L. and Sheppard, R. W. *Polymer* 1984, **25**, 369
26 Hill, R. G. *Polymer* 1985, **26**, 1708
27 Rostami, S., Ph.D. Thesis, Imperial College, London, 1983
28 Chai, Z., Ph.D. Thesis, Imperial College, London, 1982
29 Van Aartsen, J. J. *Eur. Polym. J.* 1970, **6**, 919
30 Walsh, D. J., Higgins, J. S. and Rostami, S. *Macromolecules* 1983, **16**, 388